

and density, and

$$Q(x,t) = m \int dv [v - v(x,t)]^2 f(x,v,t).$$

The field equation was solved numerically where P was obtained from (1) with $\partial Q/\partial x = 0$, i.e., in the adiabatic limit. As in the case of the simulations, the solutions showed excitations at the driving frequency and several higher harmonics. However, except for some initial transients, *there was no free-mode response*, the nonlinear convection having damped these modes out. The same result is obtained using a linearized form of Q (Landau damping). Thus we see that it is the contribution to Q due to the pulselike production of hot electrons which leads to a pressure P that ultimately acts as an additional source for the electrostatic field—an aperiodic source.

The authors gratefully acknowledge the contributions of D. F. DuBois to an early stage of this work. Helpful discussions with A. Petschek were

greatly appreciated. This work was performed under the auspices of the U. S. Department of Energy.

¹K. R. Manes *et al.*, Phys. Rev. Lett. **39**, 281 (1977); R. P. Godwin, P. Sachsenmaier, and R. Sigel, Phys. Rev. Lett. **39**, 1198 (1977).

²D. W. Forslund, J. M. Kindel, and K. Lee, Phys. Rev. Lett. **39**, 284 (1977); K. Estabrook and W. L. Kruer, Phys. Rev. Lett. **40**, 42 (1978).

³P. DeNeef and J. S. DeGroot, Phys. Fluids **20**, 1074 (1977).

⁴N. H. Burnett *et al.*, Appl. Phys. Lett. **31**, 172 (1977); E. A. McLean *et al.*, Appl. Phys. Lett. **31**, 825 (1978).

⁵C. K. Birdsall, A. B. Langdon, and H. Okuda, in *Methods in Computational Physics*, edited by B. Alder, S. Fernbach, and M. Rotenberg (Academic, New York, 1970), Vol. 9, p. 241.

Long-Time Containment of a Pure Electron Plasma

J. H. Malmberg and C. F. Driscoll

Department of Physics, University of California, San Diego, La Jolla, California 92093

(Received 15 January 1980)

A pure electron plasma has been confined in cylindrical geometry for many minutes. Confinement scalings with background pressure and magnetic field show that the maximum confinement times, while long, are 100–5000 times shorter than the limit set by electron-neutral collisions.

A single-species plasma is fundamentally different from a two-component plasma in that a single species can, in theory, be confined indefinitely. Here, we consider a cylindrical confinement geometry with an axial magnetic field. Like-particle interactions, however complex and nonlinear, cannot cause the plasma to expand radially, because the total canonical angular momentum must be conserved. Rather, it has been shown theoretically that like-particle interactions cause transport to a confined thermal equilibrium state.¹⁻⁴ Radial expansion of the plasma can occur only if external torques act to change the total canonical angular momentum. Such torques may arise from collisions with neutral atoms, angular asymmetries in the magnetic field or containment vessel, finite wall resistance, or radiation effects.

Here, we report experimental results on long-time containment of a pure electron plasma. One-half of the injected electrons are contained for

times $\tau_{1/2} \leq 350$ sec in modest magnetic fields $B \leq 676$ G, with background pressures $P \geq 10^{-10}$ Torr. The scaling of confinement time has been obtained over 7 decades in helium background pressure and $2\frac{1}{2}$ decades in B^2 . At high pressures, the containment scales as expected from transport due to electron-neutral collisions, with significant effects from Joule heating and neutral recoil cooling. At low pressures, the collisional transport time scaling is broken: The observed containment is several decades shorter than expected from binary elastic collisions alone.

The experimental configuration is shown in Fig. 1; the theory of operation has been discussed in detail elsewhere.⁵ Electrons are thermally emitted from a spiral-wound thoriated tungsten filament, which has a radially dependent potential

$$\varphi_f(r) \approx V_b + V_f r^2 / R_f^2. \quad (1)$$

For the present experiment, $V_b = -50$ V, $V_f = 12.4$ V, and the filament has radius $R_f = 1.4$ cm.

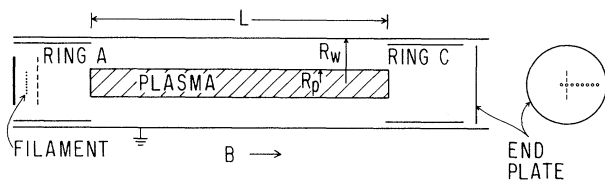


FIG. 1. The cylindrical confinement geometry.

Electrons stream along the uniform ($\pm 0.2\%$) axial magnetic field B into a grounded cylindrical tube of radius $R_w = 7.1$ cm, and are reflected by a negative potential applied to ring C at the far end. The resulting electron density is such as to give a space-charge potential $\phi_s(r) \approx \phi_f(r)$ out to the plasma edge⁵; this occurs for a density $n_0 = V_f / \pi e R_f^2 = 1.4 \times 10^7 \text{ cm}^{-3}$ which is approximately constant out to $R_p = R_f$. Measurement of the propagation of electron plasma waves has established that this type of injection results in a plasma with initial mean thermal energy $T \approx 1$ eV, giving a Debye shielding length $\lambda_D \approx 0.2$ cm.⁵

The plasma is trapped by gating ring A negative. It is held for a variable time t , then dumped axially by gating ring C to ground. The total charge remaining, $Q(t)$, is collected on the positively biased end plate, giving the particles per unit length $N(t) = -Q/eL$, where $L = 110$ cm. We also obtain the radial density profile $n(r_j, t)$ from the charges collected on Faraday cups placed behind small holes in the end plate; the holes are at radial positions $r_j = 0.83j$ cm.

Figure 2 shows the plasma evolution for $B = 676$ G and a base pressure of 1×10^{-10} Torr. The upper curve gives the line density $N(t)$ versus the hold time t , on logarithmic scales. The plasma is injected with a line density $N = 9 \times 10^7 \text{ cm}^{-1}$, and essentially no electrons are lost during the first 100 sec as the plasma expands towards the wall. In fact, N increases slightly because occasionally a background neutral is ionized: The resulting ion escapes longitudinally, but the electron is contained. By $t = 350$ sec, one-half of the electrons have been lost radially; at $t = 1000$ sec, only 10% of the electrons remain confined. The lower curves of Fig. 2 show $n(r_j, t)$ at various times. The injected plasma profile agrees closely in density and in radius with the cathode matching predictions. The central density decreases a factor of 2 in 4 sec, during which time the plasma radius increases by $\approx \sqrt{2}$. By 100 sec, the plasma extends to the wall, although electrons at $r \geq 6$ cm are not measured because they are intercepted by ring C during the dump.

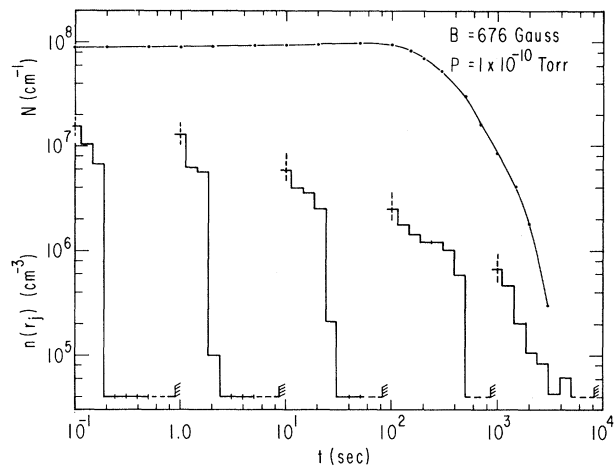


FIG. 2. Plasma evolution at base pressure and highest magnetic field. The upper curve is a log-log plot of the line density $N(t)$ vs t ; below are shown the discrete radial density profiles $n(r_j, t)$ at $t = 10^{-1}$, 1, 10, 10^2 , and 10^3 sec.

We characterize the plasma containment by the time to lose half the injected electrons, $\tau_{1/2}$; and by the time for the central density to decrease a factor of 2, τ_m . Since the total canonical angular momentum is approximately

$$\int_0^{R_w} 2\pi r dr (-eB/2c) r^2 n(r, t),$$

$\tau_{1/2}$ measures the time required for external torques to change the angular momentum by a large fixed amount, of order $(eB/2c)^{1/2} N(0) R_w^2$. The initial plasma evolution is more properly characterized by τ_m , which is also a fundamental scaling parameter of neutral transport theories.

The dependence of $\tau_{1/2}$ and τ_m on the pressure of helium gas bled into the system and on magnetic field is shown in Fig. 3. Both times scale as $P^{-1} B^2$ (shown as dashed lines) for high pressures and low magnetic fields. However, this scaling is observed to be broken in two ways. First, for low pressure, both containment times are essentially independent of pressure, and are 100–5000 times shorter than the P^{-1} projection; in this regime, $\tau_{1/2}$ scales as $B^{1.5}$, while τ_m scales as B^1 with significant irregularities in detail. Second, at high pressures and high fields, $\tau_{1/2}$ is significantly greater than expected from the B^2 scaling.

Previous pure-electron-plasma containment experiments⁵ have been dominated by electron-neutral collisional transport,⁶ and we use this as a reference for interpreting the current results. Indeed, the present device was designed to test

the extrapolation of collisional transport scaling from the 10^{-6} -Torr range of previous experiments to the 10^{-10} -Torr pressure obtainable with standard UHV technology. In the present experiments, the transport processes are slow enough that electron-electron collisions keep the velocity distribution essentially Maxwellian, and only the density and thermal energy profiles $n(r, t)$ and $T(r, t)$ need be considered. Since we use helium as a bleed gas and the electron temperature

$$\frac{\partial n}{\partial t} + \frac{1}{r} \frac{\partial}{\partial r} r \Gamma = 0, \quad (2)$$

$$\Gamma = -\frac{\partial}{\partial r} \nu r_L^2 n - \nu r_L^2 \frac{eE}{T} n, \quad (3)$$

$$\frac{\partial}{\partial t} \left(\frac{3}{2} n T \right) + \frac{1}{r} \frac{\partial}{\partial r} r \left(-\frac{\partial}{\partial r} \nu r_L^2 3 T n - \nu r_L^2 3 e E n - \frac{5}{2} \nu_{ee} r_L^2 n \frac{\partial T}{\partial r} \right) = -e E \Gamma - \frac{2m}{M} \nu \frac{3}{2} (T - T_n) n, \quad (4)$$

$$E(r) = -\frac{2e}{r} \int_0^r 2\pi r' n(r', t) dr', \quad (5)$$

with $n(R_w, t) = 0$. The electrons have thermal velocity $\bar{v} = (T/m)^{1/2}$ and Larmor radius $r_L = \bar{v} m c / e B$. The background neutrals have density n_n , mass M , thermal energy T_n , and momentum-transfer cross section σ , giving an electron-neutral collision rate $\nu = [16/3(2\pi)^{1/2}] n_n \sigma \bar{v}$. The electron-electron collision frequency is $\nu_{ee} = 16\pi^{1/2} \times e^4 n \ln \Lambda / 15 m^2 \bar{v}^3$, with $\Lambda = r_L T / e^2$.

The electric field mobility term of Eq. (3) would cause the central density of a uniform plasma to decrease a factor of 2 in a time

$$t_0 = (\nu r_L^2 / \lambda_D^2)^{-1} \propto P^{-1} B^2,$$

where $\lambda_D = (T/4\pi e^2 n)^{1/2}$ is the Debye shielding length. This is the fundamental scaling of neutral transport. When Joule-heating, diffusion-cooling, and density-gradient effects are included, numerical solutions of Eqs. (2)–(5) for our conditions predict $\tau_m = 1.5 t_0$, and $\tau_{1/2} = 9 t_0$. The dashed lines of Fig. (2) show this $P^{-1} B^2$ scaling with $\tau_{1/2} = 6 \tau_m$; the lines are normalized to the data at a single point at $B = 42$ G, $P = 6 \times 10^{-6}$ Torr. Taking $\sigma(\text{He}) = 6 \text{ \AA}^2$, the absolute agreement between theory and experiment is within the factor-of-2 uncertainty in the Bayard-Alpert ionization gauge.

The strong breaking of the P^{-1} scaling observed in experiments at low pressures could conceivably be caused by the collision frequency ν not being proportional to the gauge pressure P . This could occur if the base pressure included a component with an extraordinarily high cross section or a very low pumping rate. Two possible exam-

ples would be H_2O , with $\sigma = 3000 \text{ \AA}^2$ for room-temperature electrons,⁷ or thorium emitted from the filament, which would stick to the walls before reaching the pressure gauge. Using a residual gas analyzer, we have extensively investigated this class of effects, through heating and cooling the containment cylinder, baffling the ion pump, bleeding a variety of gases into the machine, and pulsing the filament. The anomalous loss at low pressure does not appear to be caused by an anomalously high electron-neutral collision rate.

Under these conditions, the plasma evolution is described by the particle- and energy-transport equations coupled with Poisson's equation:

The electron-electron heat-transport term in Eq. (4) also breaks the P^{-1} transport scaling, with a heat-transfer time $(\nu_{ee} r_L^2 / \lambda_D^2)^{-1} \propto B^2$. This effect will be significant on the mobility time scale when $\nu_{ee} / \nu \approx (1.5 \times 10^{-7} / P)(n / 1.4 \times 10^7) / T^2 \geq 1$, that is, for $P \leq 10^{-7}$ Torr. Although this effect becomes important at the same pressures where the experimental containment times become anomalous, we have no reason to believe the two are causally related. Numerical solutions of Eqs. (2)–(5) at $P = 6 \times 10^{-10}$ Torr do show significant effects from electron-electron heat transport: The central plasma does not cool as much because of diffusion cooling and recoil cooling, giving $\tau_m = 1 t_0$ rather than $1.5 t_0$. However, these solutions show no strong breaking of the P^{-1} scaling as is observed experimentally, since the external torque is still provided by neutral collisions. We note that this calculation does not rule out a loss mechanism which involves both electron-electron collisions and external torques

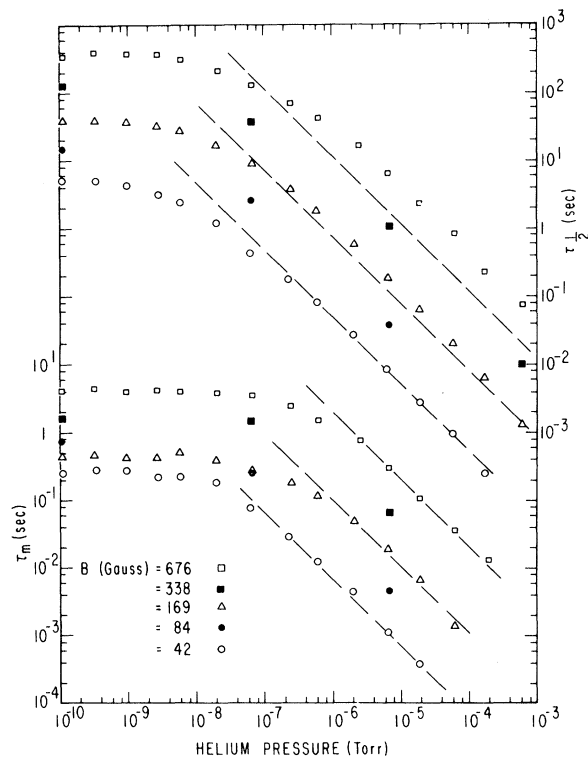


FIG. 3. Scaling of containment times with pressure for several magnetic fields. The upper curves give the time $\tau_{1/2}$ to lose one-half of the injected electrons; the lower curves give the time τ_m for the central density to decrease by a factor of 2.

from some other effect.

The neutral-recoil-cooling term in Eq. (4) breaks the basic B^2 transport scaling, with a cooling time $(\nu 2m/M)^{-1} \propto P^{-1}$. This effect will be significant on the mobility time scale when $2m/M \geq r_L^2/\lambda_D^2$, or $1 \geq (B/730)^{-2}(n/1.4 \times 10^7)$. Numerical solutions show that while τ_m is not affected for $B \leq 676$ G, $\tau_{1/2}$ is increased by factors of 1.5 and 8 at $B = 169$ and 676 G, respectively. The factor-of-8 enhancement may be an overestimate, since the numerical solutions show the electrons cooling to near room temperature, where the assumptions of our collision model break down. Nevertheless, the signature of recoil cooling is clearly seen in the data of Fig. 3: $\tau_{1/2}$ is significantly enhanced for $B \geq 169$ G, and a maximum enhancement by a factor of 4 is observed at B

= 676 G.

We do not yet know the origin of the external torque which produces the anomalous loss at low pressures. The explanation which appears most likely is that small deviations from cylindrical symmetry in the magnetic field or containment vessel modify the electron orbits, either directly or through the growth of diocotron waves. Other explanations which we consider less likely on numerical grounds include radiation effects,⁸ instabilities driven by wall resistance,⁹ and the influence of positive or negative ions formed from the background neutrals. We wish to point out, however, that this plasma is useful for studying a wide variety of plasma phenomena, even before the loss mechanism is understood.

In summary, we have verified that a pure electron plasma can be contained for many minutes at densities $n \approx 10^6 - 10^7 \text{ cm}^{-3}$ in magnetic fields $B \leq 700$ G. For helium background pressures $P \geq 10^{-6}$ Torr, containment scales as expected from neutral-transport theory, with significant cooling due to neutral recoil. For low pressures, the containment is limited by a loss mechanism which is not simply determined by elastic binary collisions.

This material is based on work supported by the National Science Foundation under Grant No. PHY 77-20613.

¹T. M. O'Neil and C. F. Driscoll, *Phys. Fluids* **22**, 266 (1979).

²A. N. Kaufman, *Phys. Fluids* **14**, 387 (1971).

³L. D. Landau and E. M. Lifshitz, *Statistical Mechanics* (Pergamon, London, 1958), Sect. 4; R. C. Davidson, *Theory of Nonneutral Plasmas* (Benjamin, Reading, Mass. 1974), Chap. 3.2.

⁴S. A. Prasad and T. M. O'Neil, *Phys. Fluids* **22**, 278 (1979).

⁵J. H. Malmberg and J. S. deGrassie, *Phys. Rev. Lett.* **35**, 577 (1975); J. S. deGrassie and J. H. Malmberg, *Phys. Rev. Lett.* **39**, 1077 (1977); J. S. deGrassie and J. H. Malmberg, *Phys. Fluids* **23**, 63 (1980).

⁶M. H. Douglas and T. M. O'Neil, *Phys. Fluids* **21**, 920 (1978).

⁷L. G. Christophorou and D. Pittman, *J. Phys. B* **3**, 1252 (1970).

⁸T. M. O'Neil, to be published.

⁹R. J. Briggs *et al.*, *Phys. Fluids* **13**, 421 (1970).